

Development and Validation of the Pyroptosis-related genes Signature for Predicting the Prognosis of Colorectal Cancer

Kexun Zhou

Sichuan University West China Hospital

Huaicheng Tan

Sichuan University West China Hospital

Ting Yu

Sichuan University West China Hospital

Chunhua Liu

Sichuan University West China Hospital

Zhenyu Ding

Sichuan University West China Hospital

Jiyan Liu

Sichuan University West China Hospital

Huashan Shi (✉ shihuashan@scu.edu.cn)

Sichuan University West China Hospital <https://orcid.org/0000-0001-8639-4677>

Primary research

Keywords: Colon Cancer, Pyroptosis, Genes Signature, Pyroptosis-related Risk Score, Prognosis

Posted Date: November 1st, 2021

DOI: <https://doi.org/10.21203/rs.3.rs-829476/v1>

License:  This work is licensed under a Creative Commons Attribution 4.0 International License.

[Read Full License](#)

Abstract

Background: Pyroptosis is an important component of the tumor microenvironment, associated with the occurrence and progression of cancer. However, the expression of pyroptosis-related genes and its impact on the prognosis of colon cancer (CC) remains unclear. Here, we constructed and validated a pyroptosis-related genes signature to predict the prognosis of patients with CC.

Methods: Public data source was obtained to screen out candidate genes for further analysis. Various methods were combined to construct a robust pyroptosis-related genes signature for predicting the prognosis of patients with CC. Based on the gene signature and clinical features, a decision tree and nomogram were developed to improve risk stratification and quantify risk assessment for individual patients.

Results: The pyroptosis-related genes signature successfully discriminated CC patients with high-risk in the training cohorts. The prognostic value of this signature was further confirmed in independent validation cohort. Multivariable Cox regression and stratified survival analysis revealed this signature was an independent prognostic factor for CC patients. The decision tree identified risk subgroups powerfully, and the nomogram incorporating the gene signature and clinical risk factors performed well in the calibration plots.

Conclusions: Pyroptosis-related genes signature was an independent prognostic factor, and can be used to predict the prognosis of patients with CC.

Background

Worldwide, colon cancer (CC) ranks the fourth most frequent cancer and the fifth leading cause of cancer death, as nearly 1.10 million newly diagnosed cases and 0.55 million deaths reported in 2018 [1]. With the development of precision medicine, significant efforts have been made to refine the personalized management of CC. Generally, treatment strategies for individual patients are mainly based on prognostic factors which have been verified in previous studies, such as the ratio of positive lymph node, the status of microsatellite instability (MSI) [2–5]. However, the value of existing prognostic markers is not sufficient. For example, it is well established that patients with stage III CC could benefit from the adjuvant therapy of fluoropyrimidines alone, as the risk of death decreases 10–15% [6]. But for stage II disease, the benefit of adjuvant chemotherapy does not improve survival by more than 5%. [7]. In addition, the predictive value of microsatellite instability (MSI) remains controversial. A retrospective study conducted by Sargent et al indicated that in stage II CC with defective DNA mismatch repair (dMMR), adjuvant therapy was associated with reduced overall survival [8]. In contrast, analyzing data from QUASAR study, Hutchins G et al found that although dMMR was prognostic, it did not predict benefit or detrimental impact of chemotherapy [9]. This finding has been borne out in another study as well [10]. Therefore, discovery of new biomarkers is required to discriminate high-risk subsets who most likely benefit from treatment and avoid unnecessary toxicities.

Pyroptosis is a form of cell death, leading to the cleavage of gasdermin D (GSDMD) and activation of inactive cytokines like IL-18 and IL-1 β [11]. Existing evidence suggests that pyroptosis plays an important role in the development of cancer cells. Kolb R summarized the role of various inflammasome factors in cancer progression and therapy. It indicated that key components of pyroptosis, such as gasdermin (GSDM) proteins and proinflammatory cytokines, are associated with tumorigenesis and invasion, as well as metastasis [12]. For example, Wei J evaluated the impact of the GSDM on the occurrence and prognosis of lung adenocarcinoma (LUAD). The results indicated that GSDMC is significantly upregulated in LUAD tissues and the overexpression of GSDMC was an independently negative prognostic factor in patients with LUAD [13]. Meanwhile, Tulotta C et al found that IL-1 β produced by breast cancer cells could promote epithelial-to-mesenchymal transition (EMT), invasion and migration. IL-1 β also caused expansion of the bone metastatic niche, which led to tumor proliferation [14]. As for CC, by knocking out the inflammatory vesicle-related genes (NLRP3 and CASP1), Dupaul-Chicoine et al found that transgenic mice were more likely to develop CCs than its counterparts [15].

Based on these findings, it is increasingly clear that pyroptosis may play an important role in the development of cancer, as well as the disease progression. However, its functional impact in CC represented a critical knowledge gap. Thus, we performed a systematic study to explore the pyroptosis-related genes for CC and the prognostic value of gene signature was validated in independent cohorts. Also, an integrated model, which was based on the gene signature and clinical features, was developed to improve the predictive power and accuracy.

Methods

Dataset

The methods have been well-established in previous studies [16, 17]. Briefly, a total of 1086 patients with CC were included in our study across different platforms. The data of gene expression was downloaded from gene expression omnibus (GEO) database. The microarray datasets GSE14333, GSE226, GSE17536, GSE177, GSE41258 and GSE250 were integrated into a new train cohort, using the sva package (COMBAT) for removing batch effects. All raw CEL files from the three datasets were downloaded and normalized using a robust multichip average (RMA) algorithm. Meanwhile, the RNA-seq data of 432 CC patients with clinical information was downloaded from The Cancer Genome Atlas (TCGA) and transcripts per million (TPM) normalized. All microarray and RNA-seq data included in our study were log2 transformed.

Development and validation of the pyroptosis-related genes prognostic model Thirty-three pyroptosis-related genes were extracted from prior reviews and presented in Table S1 [18–22]. Based on these genes, ssGSEA were used to construct the pyroptosis-related risk score (PRS). Specifically, univariate Cox proportional-hazards (Cox-PH) regression model was performed to evaluate the significance of different cancer hallmarks in CC, which was based on the R package ‘survival’. With the package of ‘wgcna’ (weighted gene co-expression network analysis), the scale-free co-expression network was performed to

identify the module which was most correlated with pyroptosis based on transcriptome profiling data and ssGSEA scores. The association of individual gene with pyroptosis ssGSEA score was quantified by Gene significance (GS), while the correlation between module eigengenes and gene expression profiles was represented by module membership (MM). Subsequently, a least absolute shrinkage and selection operator (LASSO) Cox regression model was utilized to narrow down the candidate genes, screening the most robust prognostic markers. The PRS was established as follows:

$$PRS = \sum i \text{Coefficient}(mRNA_i) \times Expression(mRNA_i)$$

The Z-score method was used to normalize ssGSEA scores and HRS when necessary. CC patients from GEO and TCGA were divided into low- and high-risk according to the risk score. Kaplan–Meier analysis with a two-sided log-rank test was employed to compare the OS between the two groups. With the R package ‘survival ROC’, time-dependent receiver operating characteristic (tROC) analysis was performed, and the areas under the curve at different time points [AUC(t)] of all the variables were compared. To evaluate the prognostic value in the pooled cohort, meta-analysis ($\hat{\rho} > 30\%$, random-effects model) was conducted. And non-negative matrix factorization (NMF) consensus clustering was used to divide one cohort without a full-scale gene signature expression pattern into different clusters according to the best k value with the R package ‘nmf’.

Independent Prognostic Analysis Of Prs

Clinical information of CC patients was extracted from the GEO and TCGA (Table S2), then analyzed in the regression model, combined with PRS. Univariate and multivariable Cox regression models were employed for the analysis. A decision tree for risk stratification with the R package ‘rpart’ was constructed, using recursive partitioning analysis (RPA). A nomogram and a calibration curve were plotted using the R package ‘rms’.

Results

Pyroptosis is the risk factor for overall survival in CC patients

The correlation heatmap containing the candidate pyroptosis-related genes is presented in Fig. 1A (red: positive correlations; blue: negative correlations). Survival-related genes were screened out by univariate Cox regression analysis. With the criteria of $P < 0.05$, 11 genes (ZBP1, SCAF11, PRKACA, NOD2, GZMA, GSDMD, CASP8, CASP5, CASP3, CASP1 and APIP). Among them, only PRKACA was associated with increased risk, as HRs > 1 , while the others were protective genes with HRs < 1 (Fig. 1B).

Based on the Z-scores of the pyroptosis ssGSEA score, 654 CC patients were divided into low- and high-risk subgroups equally. Patients with low-risk scores had a survival advantage over patients with high-risk scores (Fig. 1C). And Figure 1D shows that Z-scores of the pyroptosis ssGSEA were significantly elevated in dead patients compared with living patients during follow up. Statistical difference in overall survival (OS) was observed between two subgroups ($P < 0.0001$, Fig. 1E). As tROC demonstrated, that the area

under the ROC curve (AUC) was 0.70 for 96-month, 0.68 for 60-month, 0.68 for 36-month and 0.65 for 24-month survival (Fig. 1F).

Establishment Of Pyroptosis-related Genes Signature For Prognosis

Using whole-transcriptome profiling data and pyroptosis ssGSEA Z-scores in the training set, WGCNA was developed. Since a power of $\beta = 5$ was the optimal threshold to ensure a scale free co-expression network (supply_Fig S1), a total of 26 non-grey modules were generated (Fig. 2A). The module which was considered the most correlated with pyroptosis was represented by lightcran ($r = 0.39, p = 3e-25$) (Fig. 2B, C). Hub genes extracted from the lightcran module were used for further univariate Cox regression analysis, as a threshold of p value for GS set as <0.0001 . With a threshold of p value for uni-Cox of <0.05 , 67 potential candidates were identified (Fig. 2D). Among of them, 45 were protective markers, while 22 were risk markers. Furthermore, the most robust markers for prognosis were identified by the LASSO Cox regression model. To address the over-fitting, ten-fold cross-validation was applied, with selected optimal λ value of 0.0249 (Fig. 2E-F). After validation, with individual nonzero LASSO coefficients, CCDC88A, SYNGR1, SEPRINB9, ZAF804A, ADORA3, MYO5A, RAB38, TREM2, CTSW, CD3G, TSGA10, XCL1, CLEC2D, IL17RA, TRAF1, NCR3, KDM4A, FFAR2, IGFLR1, CD300C, IL12RB1, CYSLTR1, ACOT11, ST3GAL5, KLRD1, SLAMF1 and SOCS1 remained. The distribution of LASSO coefficients of the gene signature was presented in Fig. 2G. Finally, the PRS formula was developed as follows:

$$PRS = \sum i \text{Coefficient} (mRNA_i) \times Expression (mRNA_i)$$

The expression level of each gene was log2 normalized.

PRS is an accurate predictor for overall survival of CC patients

The prognostic value of PRS was validated in the training set. Using the 33-gene set of pyroptosis reported in previous studies, GSEA confirmed the difference of gene set enrichment in the two subgroups, since risk markers positively correlated with pyroptosis accumulated more in the high-PRS group, compared with the low-PRS group (Fig. 3A). Furthermore, the follow-up data indicated that the risk score significantly decreased in patients alive (Fig. 3B). As Kaplan–Meier survival curve indicated, patients with lower PRS enjoyed a statistically significant survival benefit than its competitor ($p < 0.0001$, Fig. 3C). Since various clinicopathological factors were included in multivariate Cox regression model of the training cohort, the results revealed that TNM stage (HR = 1.8732, $p < 0.1$) and PRS (HR = 4.302, $p < 0.1$) were two independent risk factors for OS (Fig. 3D). In addition, tROC analysis suggested that PRS was an accurate variable for predicting the survival of CC patients (Fig. 3E).

The robustness of predictive value of the pyroptosis-related genes signature was validated in other independent external cohorts. Briefly, by using TCGA, higher enrichment score of pyroptosis gene set was confirmed in the high-PRS group in the validation I cohort (Fig. 4A). Also, patients alive had lower PRS, compared with deceased patients ($p < 0.0001$, Fig. 4B). Kaplan–Meier analysis confirmed the survival

benefit in patients with lower PRS in the validation cohort ($p<0.0001$, Fig. 4C). Furthermore, NMF consensus clustering was used to divide both TCGA and GEO cohort into two groups (Fig. 4D, E). The division was based on the best k value, which was the remaining expression pattern of the gene signature. The results revealed statistical difference in OS between NMF-derived groups (Fig. 4F, G). Moreover, multivariate Cox regression analysis indicated that not only in the training and validation cohort, PRS was an independent risk factor for OS (Fig. 4H), but also in the all cohorts (Fig. 4I).

PRS acts as an indicator of worse prognosis in the pooled cohort and a promising marker of therapeutic resistance.

To evaluate the prognostic value of the pyroptosis-related genes signature in the pooled cohort including the training and validation cohorts, meta-analysis was performed. The results suggested that CC patients with higher PRS had worse prognosis than those with lower PRS (pooled Hazard Ration (HR) = 2.63, 95% CI 2.07–3.35) (Fig. 5A, B). Subsequently, 1096 patients were extracted for further investigation. PRS Z-scores were significantly elevated in those patients who died during the follow-up, especially in patients with shorter survival (Fig. 5C). When the candidate patients were divided into different subgroups, according to virous clinicopathological features (age, sex and stage), PRS also helped to screen out high-risk patients with poor prognosis (Fig. 5D).

Since limited evidence can be reached, we tried to explore whether the pyroptosis-related genes signature is a marker of chemotherapy resistance, as well as recurrence. As shown in Fig. 6A, GSEA confirmed that higher PRS is not only significantly associated with resistance to chemotherapy drugs, including cisplatin and fluorouracil, but also with disease recurrence. Further functional assays indicated that PRS is negatively associated with virous cancer therapeutic pathways, which have been validated in previous study [23] (Fig. 6B). However, PRS is related to immunosuppressive cells, such as Treg. In contrast, it is negatively associated with T cell (Fig. 6C). Furthermore, by using GSCALite, a landscape plot was generated to depict the relationships between the response to targeted drugs and pyroptosis-related genes signature expression (Fig. 6C). The results presented as the bubble heatmap were consistent with that of LASSO coefficients (Fig. 2C). Specially, CCDC88A was associated with multi-drug resistance, while RAB38, CYSLTR1 exhibited drug sensitivity. Medical information from TCGA were used to validate the prediction. As Fig. 6D shown, although statistical difference was not reached, the disease control rate (DCR) was much higher in patients with low-PRS, compared with its competitor (88 vs 83%, $p=0.092$). Moreover, low-PRS is a prognostic marker of a more favorable outcome among CC patients who received anti-cancer drugs ($p = 0.032$) (Fig. 6E) or surgery ($p = 0.026$) (Fig. 6F). When patients were stratified by the location of tumor, low-PRS group still had a survival advantage over high-PRS group ($p<0.0001$) (Fig. 6G).

Combination of the pyroptosis signature and clinicopathological features improves risk stratification and survival prediction

A decision tree improving risk stratification for OS was constructed, as 1096 patients with four parameters available, age (>70 or ≤ 70), sex (male or female), TNM stage ($<\text{IV}$ or $\geq \text{IV}$) and PRS (low or

high) were included. The results indicated that only TNM stage and PRS remained, as three different risk subgroups was identified (Fig. 7A). Furthermore, in the node of stage <IV, PRS replaced TNM stage. Kaplan–Meier analysis indicated that statistical difference of OS was reached among the three risk subgroups ($p<0.0001$) (Fig. 7B).

A nomogram with PRS combined with other clinicopathological features was developed, aiming to quantify the risk assessment and survival probability for individual CC patients (Fig. 7C). In the calibration analysis, all the prediction lines (red, blue and purple line represented 8-year, 5-year, 3-year survival) of the nomogram were close to the ideal performance (45-degree dotted line) (Fig. 7D), validating the accuracy of the nomogram. As shown in Fig. 7E, tROC analysis indicated that nomogram had the most powerful predictive ability, as the clinical benefit of the nomogram has been demonstrated in decision curve analysis (DCA) (Fig. 7F).

Discussion

In current study, using public data source, we firstly identified pyroptosis is a risk factor for OS in CC patients. Then combined methods were used to construct a pyroptosis-related genes prognostic model. The prognostic value of PRS, derived from the gene signature, was validated in independent cohorts. Further analysis suggested that PRS could be served as an independent risk factor to identify patient population with high-risk. Functional analyses indicated that PRS is negatively associated with virous pathways, such as cell cycle and p53 signaling pathway, but related to immunosuppressive cells, such as Treg.

Pyroptosis, an inflammatory type of regulated cell death, is characterized by cell swelling, lysis, and the release of many proinflammatory factors, such as IL-1 β and IL-18 [20]. In the past decade, the relationship between pyroptosis and cancer have attracted widespread attention. Existing evidence suggested that pyroptosis may impact the proliferation, invasion, and metastasis of tumor, making it a promising therapeutic target [21, 22, 24]. Also, some individual pyroptosis genes have been studied in various cancer types, such as NOD2 in colorectal cancer [25, 26], Gasdermin D (GSDMD) in gastric cancer [27], and gasdermin B (GSDMB) in digestive system [28]. However, current studies are clearly inadequate. To date, how pyroptosis-related genes interact and whether they are related to the survival of patients with cancer remain little known. Only a study was powered by Ye Y et al, aiming to address this question in patients with ovarian cancer. Using data from TCGA cohort, a multigene signature was constructed to evaluate the prognostic value of pyroptosis-related genes in this patient population and was further validated in GEO cohort [29]. The results confirmed that prognostic value of pyroptosis-related genes in patients with ovarian cancer. But the influence of these gene signatures may vary for different types of cancer. Thus, it is worthy to establish a pyroptosis-related risk score for patients with CC, providing evidence of prognostic value.

Unlike 7-gene risk signature constructed by Ye Y et al [29], we established a 27-gene signature, which was derived from LASSO Cox regression model. Among those genes, few of them showed evident correlations

with cancer or pyroptosis in previous studies. The protective value of ACOT11, ST3GAL5, and SERPINB9 has been validated in renal cell carcinoma, bladder cancer and colorectal cancer [30–32], while MYO5A, RAB38, and CYSLTR1 were involved in the progression of various cancer type, such as gastric cancer, pancreatic cancer, and non-small cell lung cancer [33–36]. As for SOCS1, a biomarker with the largest protective coefficient in our study, is widely recognized as a tumor suppressor. However, its role in CRC remains controversial. Hanada T et al found that SOCS1 is a tumor suppressor which could prevents chronic inflammation-mediated carcinogenesis by regulation of the IFN gamma/STAT1 pathways [37]. Inconsistent with this finding, study conducted by Tobelaim WS et al indicated that SOCS1 may work as an oncogene in CRC [38]. In summary, the biological functions associated with tumor pyroptosis of the novel gene signature still require further investigation in CC.

After the selection of pyroptosis-related genes signature, the risk score, decision tree and the nomogram were constructed. The methods were well-established in previous studies. Aiming to develop a hypoxia-based method to identify patients with high-risk in early-stage lung adenocarcinoma (LUAD), Sun J et al used combined methods to screen for robust biomarkers and establish a hypoxia-related gene signature for prognosis. The prognostic value of the gene signature was further validated by the decision tree and the nomogram, confirming that the hypoxia-related gene signature could discriminated patients with high-risk in early-stage LUAD powerfully [16]. In addition, Ye Y et al used similar methods to establish a novel defined pyroptosis-related genes signature to predict the prognosis of ovarian cancer [29]. The application of univariate and multivariable Cox regression analyses confirmed that the risk score was a prognostic factor.

Again, our results indicated that this combined method is a useful tool to develop and validate of the pyroptosis-related genes prognostic model in CC patients. Patients with lower PRS had favorable survival compared with those with higher PRS, which was confirmed in training and validation sets. Potential reason could be derived from our study, as higher PRS is significantly associated with resistance to chemotherapy drugs, as well as the disease recurrence. Previous studies have been powered to investigate the involvement of pyroptosis in cancer treatment [39, 40]. For example, Wang X et al found that the treatment of Taxol caused pyroptotic death in nasopharyngeal cancer cell line, which was mediated by Caspase-1 and GSDMD [39]. Meanwhile, based on a series of experiments conducted by Westbom C et al, the results suggested that doxorubicin and cisplatin could activate Caspase-1 and pyroptosis, which contributed to the death of cancer cells [40]. As for our findings, the pyroptosis-related genes signature-derived resistance to therapies, need to be conquered by further studies.

Although pyroptosis has not been fully studied, significant efforts have been made to identify the impact of pyroptosis on tumor immune microenvironment. Study conducted by Wang Q et al suggested tumor-suppressed immune cells are recruited by tumor cells undergoing pyroptosis [41], which was in line with the simultaneously published study performed by Zhang Z et al [42]. Meanwhile, Wang et al. found that only in the context of the concomitant induction of pyroptosis, immunotherapy could efficiently kill a specific group of tumor cells, which showed natural resistance to immunotherapy [41]. In addition, based on the results of Gene Ontology (GO) and Kyoto Encyclopedia of Genes and Genomes (KEGG) analyses, Ye

Y et al proposed that pyroptosis could regulate the composition of the tumor immune microenvironment [29]. Interestingly, after stratified by PRS, Ye Y et al found that higher proportion of Treg was found in the low-risk group. As Treg was redeemed as immunosuppressive and associated with poor outcomes, possible reason for this discrepancy may be that the regulation of the overactive inflammatory reaction caused by pyroptosis requires Treg. In our study, functional assays indicated PRS is closely related to immunosuppressive cells, including Treg. Notably, Saito T identified two main subtypes of Treg in colon cancers, which had opposite roles in the regulation of the tumor microenvironment [43]. Therefore, it is worthy to further identify the specific subtype of Treg correlated to PRS.

To our best knowledge, this is the first study to explore the pyroptosis-related genes for CC patients. A pyroptosis -related risk score (PRS) was established and furtherly validated in independent cohorts. However, this study is limited by its retrospective nature. As little evidence could be reached, our findings should be conquered by further experimental studies. And the molecular mechanism also needs to be furtherly addressed.

Conclusions

In summary, we established a pyroptosis-related genes signature to discriminate CC patients with different risk and predict the survival outcomes of this patient population. Further decision tree and nomogram confirmed the predictive value of pyroptosis-related genes signature. Our model could be a useful tool to select high-risk CC patients and facilitate individual management of CC.

Abbreviations

CC
colon cancer
MSI
microsatellite instability
dMMR
defective DNA mismatch repair
GSDMD
gasdermin D
GSDM
gasdermin
LUAD
lung adenocarcinoma
EMT
epithelial-to-mesenchymal transition
GEO
gene expression omnibus
RMA

robust multichip average

TCGA

The Cancer Genome Atlas

TPM

transcripts per million

PRS

pyroptosis-related risk score

Cox-PH

Cox proportional-hazards

GS

Gene significance

MM

module membership

LASSO

least absolute shrinkage and selection operator

tROC

time-dependent receiver operating characteristic

AUC(t)

areas under the curve at different time points

NMF

non-negative matrix factorization

OS

overall survival

Declarations

Ethics approval and consent to participate: This study was approved by the Institutional Ethics Review Board of West China Hospital, Sichuan University.

Consent for publication: Not applicable

Availability of data and materials: The datasets used and/or analyzed during the current study are available from the corresponding author on reasonable request.

Competing interests: The authors declare that they have no competing interests.

Funding: This work was financially supported by the National Natural Science Foundation of China (Grant No. 82003195), and the China Postdoctoral Science Foundation (Grant No.2020M680150).

Author Contribution Statement: K.Z. performed the literature search and bioinformatics analysis; H.T. participated in the bioinformatics analysis and wrote the original draft; T.Y., C.L., Z.D. and J.L. helped with

the data collection and analysis; H.S. conceived the study, helped with data analysis and interpretation, and revised the manuscript. All the authors read and approved the final manuscript.

Acknowledgements: The authors would like to thank TCGA (<http://cancergenome.nih.gov>) for data collection, and the TIMER (<https://cistrome.shinyapps.io/timer>) for the provision of data processing and customizable functions.

References

1. Bray F, Ferlay J, Soerjomataram I, Siegel RL, Torre LA, Jemal A. Global cancer statistics 2018: GLOBOCAN estimates of incidence and mortality worldwide for 36 cancers in 185 countries. *CA Cancer J Clin.* 2018 Nov;68(6):394–424.
2. Gill S, Haince JF, Shi Q, Pavey ES, Beaudry G, Sargent DJ, et al. Prognostic Value of Molecular Detection of Lymph Node Metastases After Curative Resection of Stage II Colon Cancer: A Systematic Pooled Data Analysis. *Clin Colorectal Cancer.* 2015 Jun;14(2):99–105.
3. Sabbagh C, Mauvais F, Cosse C, Rebibo L, Joly JP, Dromer D, et al. A lymph node ratio of 10% is predictive of survival in stage III colon cancer: a French regional study. *Int Surg.* 2014 Jul-Aug;99(4):344–53.
4. Ribic CM, Sargent DJ, Moore MJ, Thibodeau SN, French AJ, Goldberg RM, et al. Tumor microsatellite-instability status as a predictor of benefit from fluorouracil-based adjuvant chemotherapy for colon cancer. *N Engl J Med.* 2003 Jul 17;349(3):247–57.
5. Sargent DJ, Marsoni S, Monges G, Thibodeau SN, Labianca R, Hamilton SR, et al. Defective mismatch repair as a predictive marker for lack of efficacy of fluorouracil-based adjuvant therapy in colon cancer. *J Clin Oncol.* 2010 Jul 10;28(20):3219–26.
6. Twelves C, Wong A, Nowacki MP, Abt M, Burris H 3rd, Carrato A, et al. Capecitabine as adjuvant treatment for stage III colon cancer. *N Engl J Med.* 2005 Jun 30;352(26):2696–704.
7. Quasar Collaborative Group, Gray R, Barnwell J, McConkey C, Hills RK, Williams NS, et al. Adjuvant chemotherapy versus observation in patients with colorectal cancer: a randomised study. *Lancet.* 2007 Dec 15;370(9604):2020–9.
8. Sargent DJ, Marsoni S, Monges G, Thibodeau SN, Labianca R, Hamilton SR, et al. Defective mismatch repair as a predictive marker for lack of efficacy of fluorouracil-based adjuvant therapy in colon cancer. *J Clin Oncol.* 2010 Jul 10;28(20):3219–26. doi: 10.1200/JCO.2009.27.1825. Epub 2010 May 24. Erratum in: *J Clin Oncol.* 2010 Oct 20;28(30):4664.
9. Hutchins G, Southward K, Handley K, Magill L, Beaumont C, Stahlschmidt J, et al. Value of mismatch repair, KRAS, and BRAF mutations in predicting recurrence and benefits from chemotherapy in colorectal cancer. *J Clin Oncol.* 2011 Apr 1;29(10):1261–70. doi: 10.1200/JCO.2010.30.1366. Epub 2011 Mar 7. Erratum in: *J Clin Oncol.* 2011 Jul 20;29(21):2949.
10. Bertagnolli MM, Redston M, Compton CC, Niedzwiecki D, Mayer RJ, Goldberg RM, et al. Microsatellite instability and loss of heterozygosity at chromosomal location 18q: prospective evaluation of

- biomarkers for stages II and III colon cancer—a study of CALGB 9581 and 89803. *J Clin Oncol.* 2011 Aug 10;29(23):3153-62.
11. Fang Y, Tian S, Pan Y, Li W, Wang Q, Tang Y, et al. Pyroptosis: A new frontier in cancer. *Biomed Pharmacother.* 2020 Jan; 121:109595.
 12. Kolb R, Liu GH, Janowski AM, Sutterwala FS, Zhang W. Inflammasomes in cancer: a double-edged sword. *Protein Cell.* 2014 Jan;5(1):12–20.
 13. Wei J, Xu Z, Chen X, Wang X, Zeng S, Qian L, et al. Overexpression of GSDMC is a prognostic factor for predicting a poor outcome in lung adenocarcinoma. *Mol Med Rep.* 2020 Jan;21(1):360–370.
 14. Tulotta C, Lefley DV, Freeman K, Gregory WM, Hanby AM, Heath PR, et al. Endogenous Production of IL1B by Breast Cancer Cells Drives Metastasis and Colonization of the Bone Microenvironment. *Clin Cancer Res.* 2019 May 1;25(9):2769-2782.
 15. Dupaul-Chicoine J, Yeretssian G, Doiron K, Bergstrom KS, McIntire CR, LeBlanc PM, et al. Control of intestinal homeostasis, colitis, and colitis-associated colorectal cancer by the inflammatory caspases. *Immunity.* 2010 Mar 26;32(3):367–78.
 16. Sun J, Zhao T, Zhao D, Qi X, Bao X, Shi R, et al. Development and validation of a hypoxia-related gene signature to predict overall survival in early-stage lung adenocarcinoma patients. *Ther Adv Med Oncol.* 2020 Jul 2; 12:1758835920937904.
 17. Irizarry RA, Hobbs B, Collin F, Beazer-Barclay YD, Antonellis KJ, Scherf U, et al. Exploration, normalization, and summaries of high density oligonucleotide array probe level data. *Biostatistics.* 2003 Apr;4(2):249–64.
 18. Barbie DA, Tamayo P, Boehm JS, Kim SY, Moody SE, Dunn IF, et al. Systematic RNA interference reveals that oncogenic KRAS-driven cancers require TBK1. *Nature.* 2009 Nov 5;462(7269):108–12.
 19. Liberzon A, Subramanian A, Pinchback R, Thorvaldsdóttir H, Tamayo P, Mesirov JP. Molecular signatures database (MSigDB) 3.0. *Bioinformatics.* 2011 Jun 15;27(12):1739–40.
 20. Tang R, Xu J, Zhang B, Liu J, Liang C, Hua J, et al. Ferroptosis, necroptosis, and pyroptosis in anticancer immunity. *J Hematol Oncol.* 2020; 10;13(1):110.
 21. Akiyama T, Inamori M, Iida H, Endo H, Hosono K, Sakamoto Y, et al. Shape of Barrett's epithelium is associated with prevalence of erosive esophagitis. *World J Gastroenterol.* 2010; 28;16(4):484–9.
 22. So D, Shin HW, Kim J, Lee M, Myeong J, Chun YS, et al. Cervical cancer is addicted to SIRT1 disarming the AIM2 antiviral defense. *Oncogene.* 2018; 37(38):5191–5204.
 23. Hu J, Yu A, Othmane B, Qiu D, Li H, Li C, et al. Siglec15 shapes a non-inflamed tumor microenvironment and predicts the molecular subtype in bladder cancer. *Theranostics.* 2021;11(7):3089–3108.
 24. Awad F, Assrawi E, Louvrier C, Jumeau C, Giurgea I, Amselem S, et al. Photoaging and skin cancer: Is the inflammasome the missing link? *Mech Ageing Dev.* 2018; 172:131–137.
 25. Couturier-Maillard A, Secher T, Rehman A, Normand S, De Arcangelis A, Haesler R, et al. NOD2-mediated dysbiosis predisposes mice to transmissible colitis and colorectal cancer. *J Clin Invest.*

- 2013;123(2):700–11.
26. Branquinho D, Freire P, Sofia C. NOD2 mutations and colorectal cancer - Where do we stand? *World J Gastrointest Surg.* 2016; 27;8(4):284-93.
 27. Wang WJ, Chen D, Jiang MZ, Xu B, Li XW, Chu Y, et al. Downregulation of gasdermin D promotes gastric cancer proliferation by regulating cell cycle-related proteins. *J Dig Dis.* 2018;19(2):74–83.
 28. Zhou Z, He H, Wang K, Shi X, Wang Y, Su Y, et al. Granzyme A from cytotoxic lymphocytes cleaves GSDMB to trigger pyroptosis in target cells. *Science.* 2020; 29;368(6494): eaaz7548.
 29. Ye Y, Dai Q, Qi H. A novel defined pyroptosis-related gene signature for predicting the prognosis of ovarian cancer. *Cell Death Discov.* 2021; 7;7(1):71.
 30. Vycital O, Pitule P, Hosek P, Kriz T, Treska V, Liska V. Expression of Serpin B9 as a Prognostic Factor of Colorectal Cancer. *Anticancer Res.* 2019; 39(11):6063–6066.
 31. Xu CL, Chen L, Li D, Chen FT, Sha ML, Shao Y. Acyl-CoA Thioesterase 8 and 11 as Novel Biomarkers for Clear Cell Renal Cell Carcinoma. *Front Genet.* 2020; 10; 11:594969.
 32. Ouyang S, Liu JH, Ni Z, Ding GF, Wang QZ. Downregulation of ST3GAL5 is associated with muscle invasion, high grade and a poor prognosis in patients with bladder cancer. *Oncol Lett.* 2020;20(1):828–840.
 33. Lan L, Han H, Zuo H, Chen Z, Du Y, Zhao W, et al. Upregulation of myosin Va by Snail is involved in cancer cell migration and metastasis. *Int J Cancer.* 2010; 1;126(1):53-64.
 34. Li BY, He LJ, Zhang XL, Liu H, Liu B. High expression of RAB38 promotes malignant progression of pancreatic cancer. *Mol Med Rep.* 2019;19(2):909–918.
 35. Hsieh JJ, Hou MM, Chang JW, Shen YC, Cheng HY, Hsu T. *RAB38* is a potential prognostic factor for tumor recurrence in non-small cell lung cancer. *Oncol Lett.* 2019;18(3):2598–2604.
 36. Ohd JF, Nielsen CK, Campbell J, Landberg G, Löfberg H, Sjölander A. Expression of the leukotriene D4 receptor CysLT1, COX-2, and other cell survival factors in colorectal adenocarcinomas. *Gastroenterology.* 2003;124(1):57–70.
 37. Hanada T, Kobayashi T, Chinen T, Saeki K, Takaki H, Koga K, et al. IFNgamma-dependent, spontaneous development of colorectal carcinomas in SOCS1-deficient mice. *J Exp Med.* 2006;12;203(6):1391–7.
 38. Tobelaim WS, Beaurivage C, Champagne A, Pomerleau V, Simoneau A, Chababi W, et al. Tumour-promoting role of SOCS1 in colorectal cancer cells. *Sci Rep.* 2015;22; 5:14301.
 39. Wang X, Li H, Li W, Xie J, Wang F, Peng X, et al. The role of Caspase-1/GSDMD-mediated pyroptosis in Taxol-induced cell death and a Taxol-resistant phenotype in nasopharyngeal carcinoma regulated by autophagy. *Cell Biol Toxicol.* 2020; 36(5):437–457.
 40. Westbom C, Thompson JK, Leggett A, MacPherson M, Beuschel S, Pass H, et al. Inflammasome Modulation by Chemotherapeutics in Malignant Mesothelioma. *PLoS One.* 2015; 21;10(12): e0145404.

41. Wang Q, Wang Y, Ding J, Wang C, Zhou X, Gao W, et al. A bioorthogonal system reveals antitumour immune function of pyroptosis. *Nature*. 2020; 579(7799):421–426.
42. Zhang Z, Zhang Y, Xia S, Kong Q, Li S, Liu X, et al. Gasdermin E suppresses tumour growth by activating anti-tumour immunity. *Nature*. 2020; 579(7799):415–420.
43. Saito T, Nishikawa H, Wada H, Nagano Y, Sugiyama D, Atarashi K, et al. Two FOXP3(+) CD4(+) T cell subpopulations distinctly control the prognosis of colorectal cancers. *Nat Med*. 2016; 22(6):679–84.

Figures

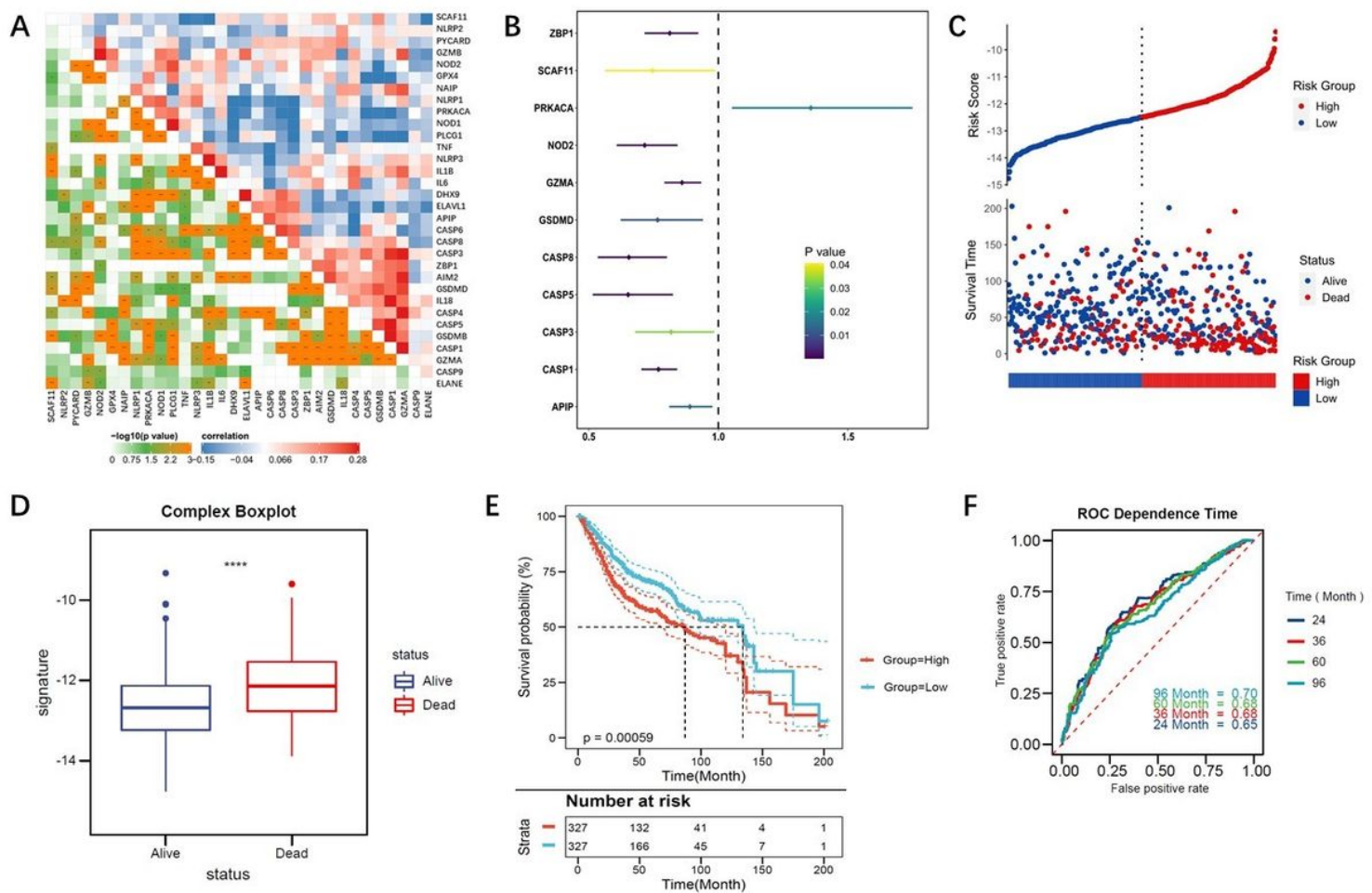


Figure 1

Identify the pyroptosis-related genes. (A) The correlation heatmap containing the candidate pyroptosis-related genes. (Red: positive correlation; Blue: negative correlation. The strength of the relevance was represented by the depth of the color) (B) Univariate cox regression analysis of OS for each pyroptosis-related genes. (C) Patients with low-risk scores had a survival advantage over patients with high-risk scores. (D) Pyroptosis ssGSEA scores were significantly elevated in patients who died during follow up. (E) Kaplan–Meier curves for the OS of patients in the high- and low-risk groups. (F) ROC curves indicated the predictive efficiency of the risk score.

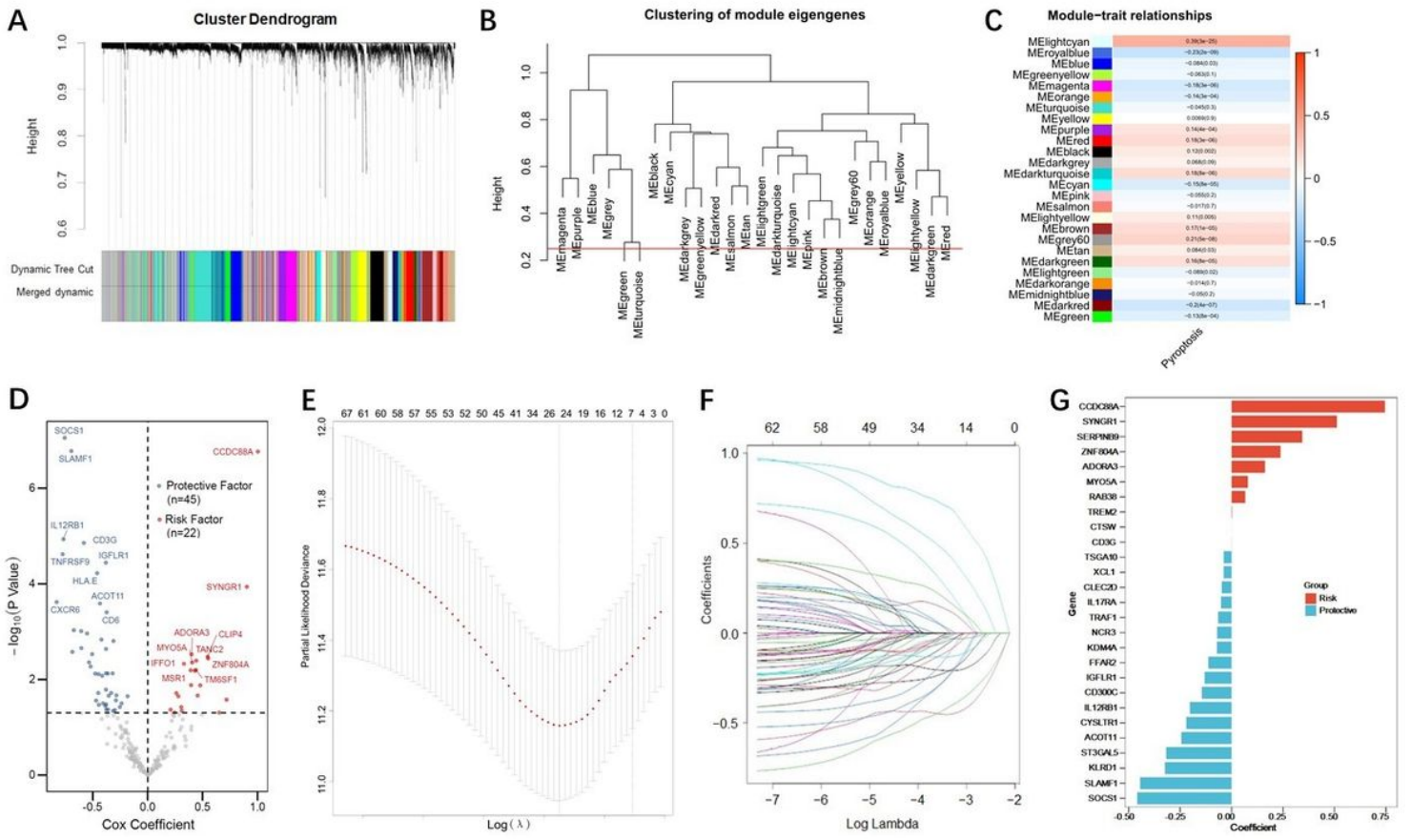


Figure 2

Construction of risk signature in the training cohort (A) WGCNA was performed with whole-transcriptome profiling data and pyroptosis ssGSEA Z-score. (B) A total of 26 non-grey modules were identified after merging. (C) The red module depicting the highest correlation ($r = 0.18$, $p = 3e-06$) was considered the most correlated with pyroptosis. (D) Sixty-seven promising candidates were identified among hub genes extracted from the red module. (E-F) The LASSO Cox regression model was used to identify the most robust markers, with an optimal λ value of 0.0617. (G) Distribution of LASSO coefficients of the pyroptosis-related gene signature.

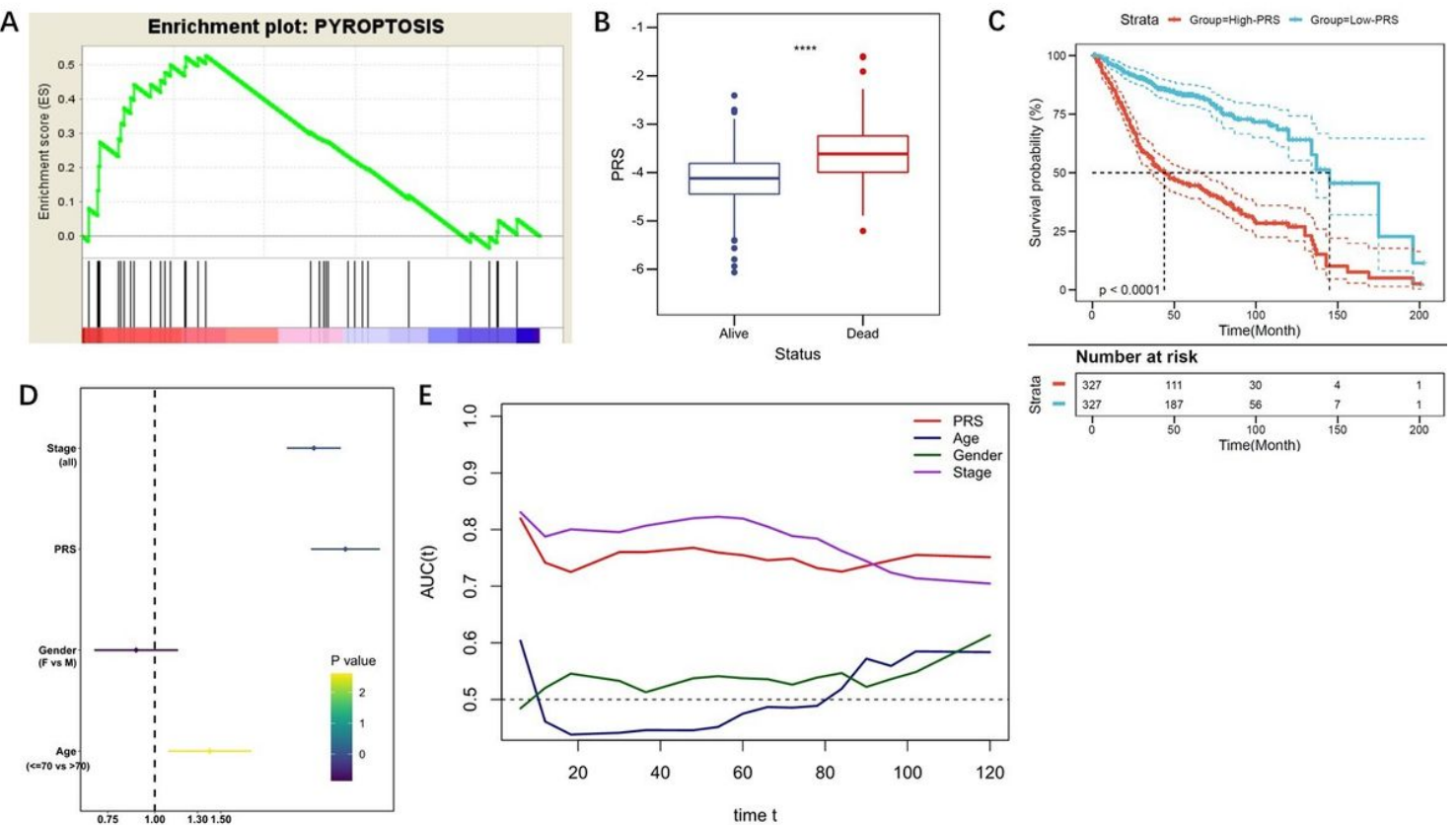


Figure 3

The gene signature predicts worse survival in the training set. (A) GSEA confirmed the status of pyroptosis in the two subgroups (B) The follow up data indicated that PRS significantly decreased in patients alive. (C) Kaplan–Meier survival curve showed that patients with lower PRS enjoyed better outcomes. (D) Multivariate Cox regression analysis demonstrated that PRS was an independent risk factor for OS. (E) tROC analysis suggested that PRS was an accurate variable for predicting the survival.

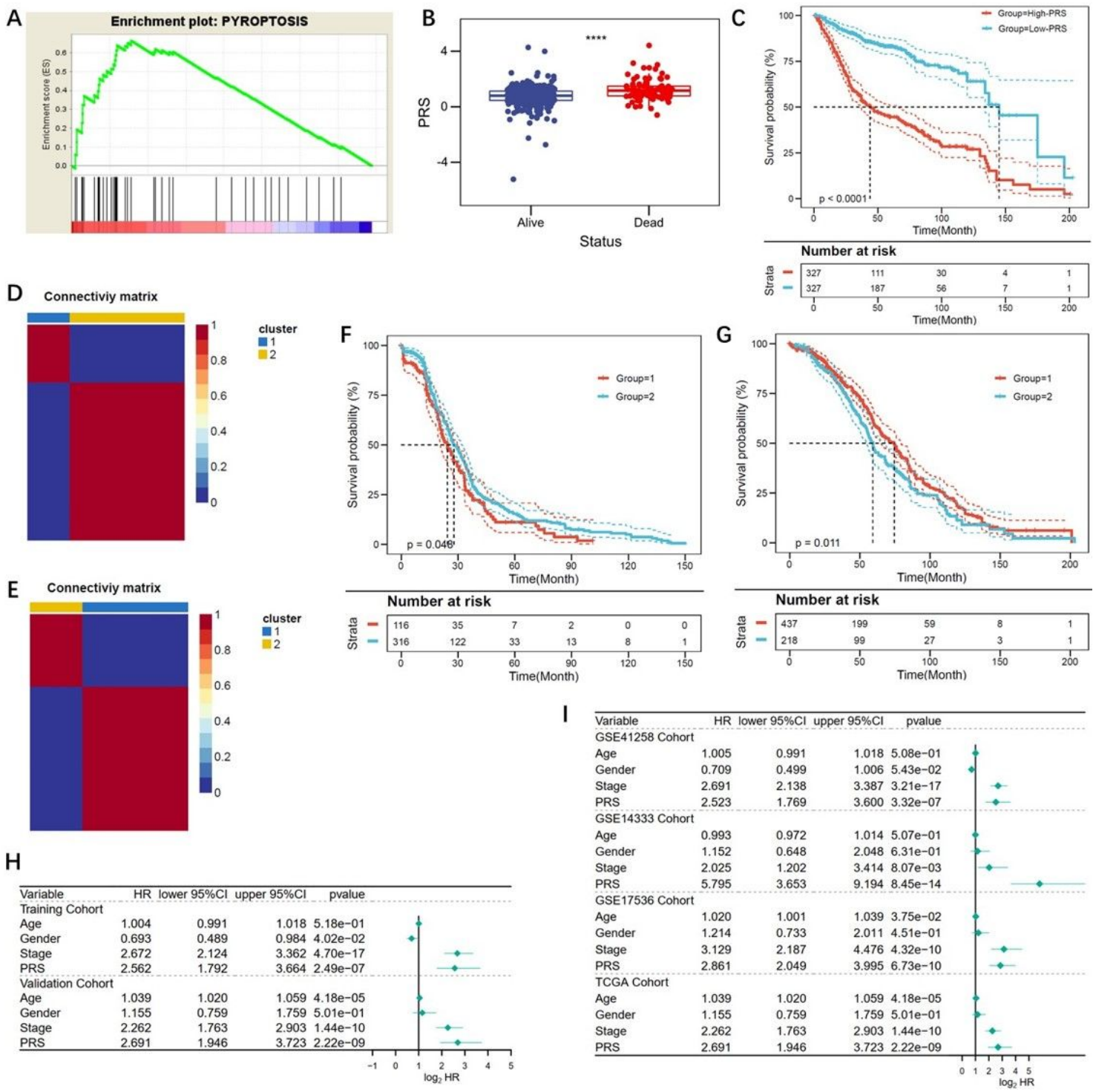


Figure 4

Validation of the gene signature in different series (A) TCGA confirmed the pyroptosis status in the validation cohort. (B) PRS was significantly decreased in patients alive in the validation cohort. (C) Patients with lower PRS exhibited better prognosis in the validation cohort. (D, E) The best k value was chosen for NMF consensus clustering in the TCGA (Fig 4D) and GEO (Fig 4E) cohorts. (F, G) Statistical difference in OS was observed in NMF-derived clusters based on the expression pattern of the gene signature (TCGA: Fig 4F; GEO: Fig 4G). (H, I) Multivariate Cox regression analysis indicated that PRS was

an independent risk factor for OS in the training and validation cohorts (Fig 4H), as well as in the all cohorts (Fig 4I).

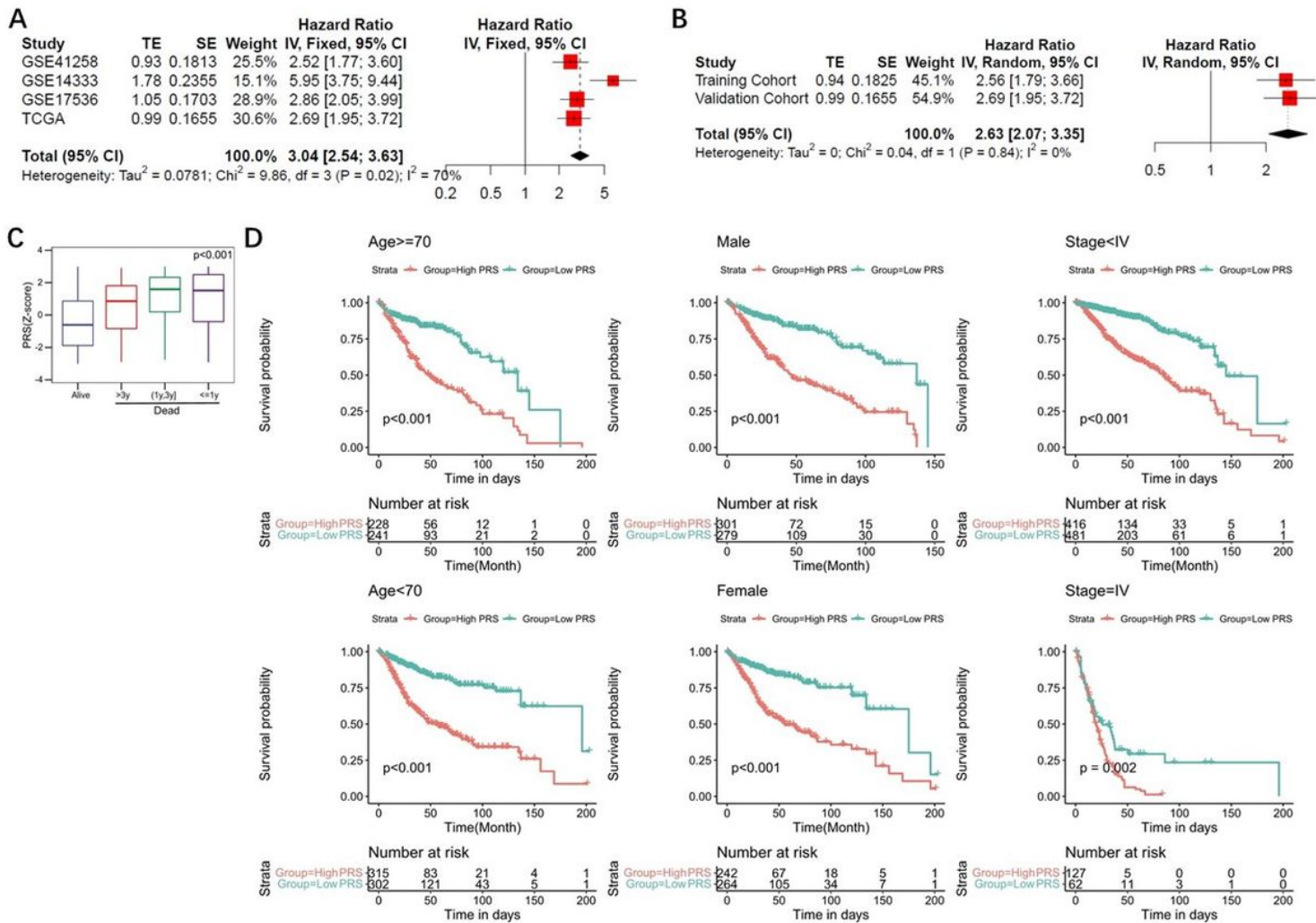


Figure 5

The gene signature serves as a valuable marker for poor survival in the pooled cohort. (A) Meta-analysis in the training and validation cohorts. (B) Meta-analysis for subgroup analysis. (C) PRS Z-scores were significantly elevated in deceased patients. (D) PRS discriminated high-risk patients in different clinicopathological including gender, age, and p-stage.

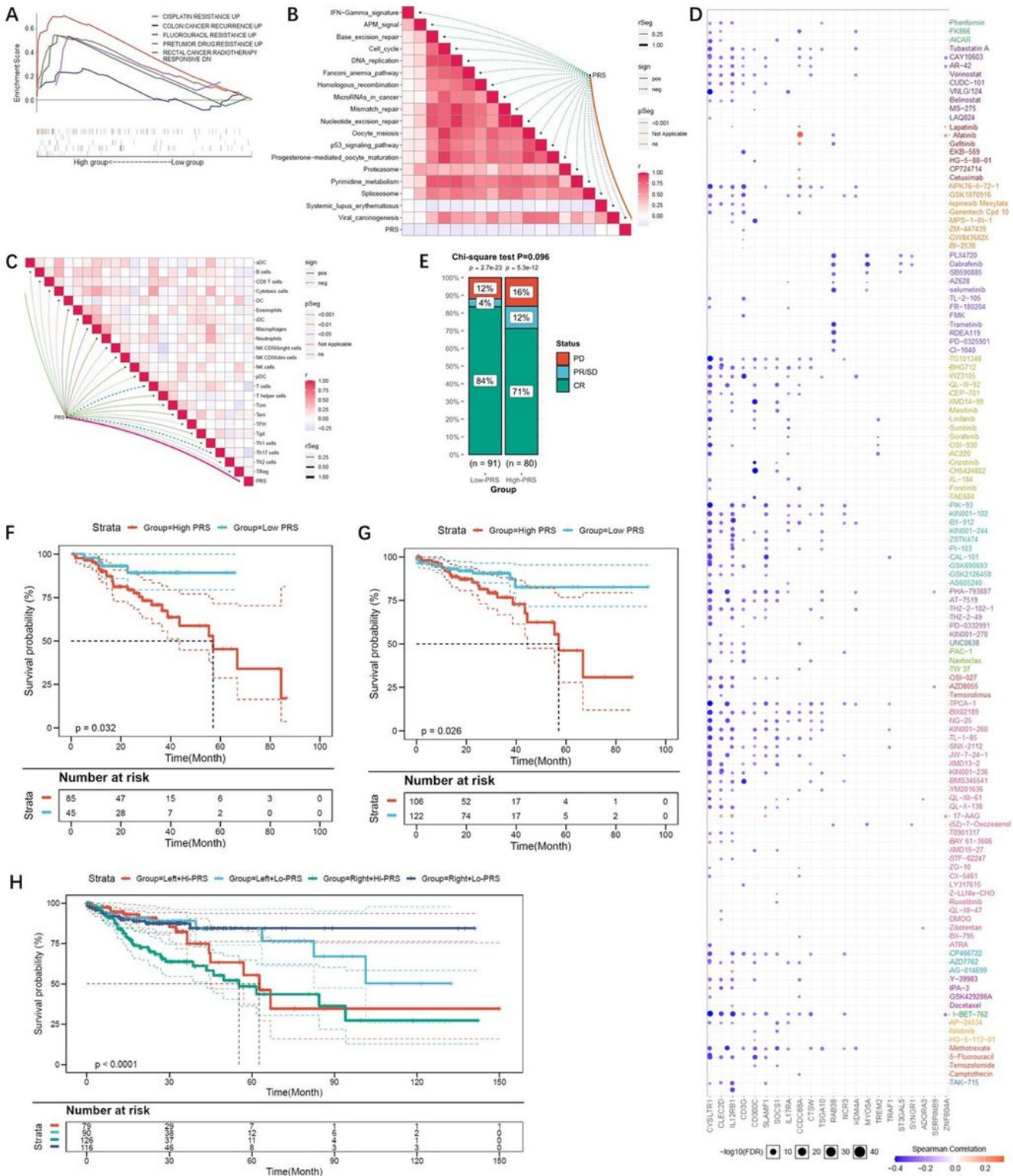


Figure 6

The pyroptotic-related gene signature is a promising marker of therapeutic resistance. (A) GSEA confirmed that the gene signature was associated with therapeutic resistance. (B) PRS is negatively associated with virous cancer therapeutic pathways. (C) PRS is related to immunosuppressive cells. (D) A landscape plot was conducted to depict the relationships between different molecules and the pyroptosis-related gene signature. (E) The ratio of worse outcomes after surgery is greatly elevated in

higher PRS group. (F-H) Low-PRS is a prognostic marker of a more favorable outcome in different subgroups (6F: drugs; 6G: surgery; 6H: location of primary tumor).

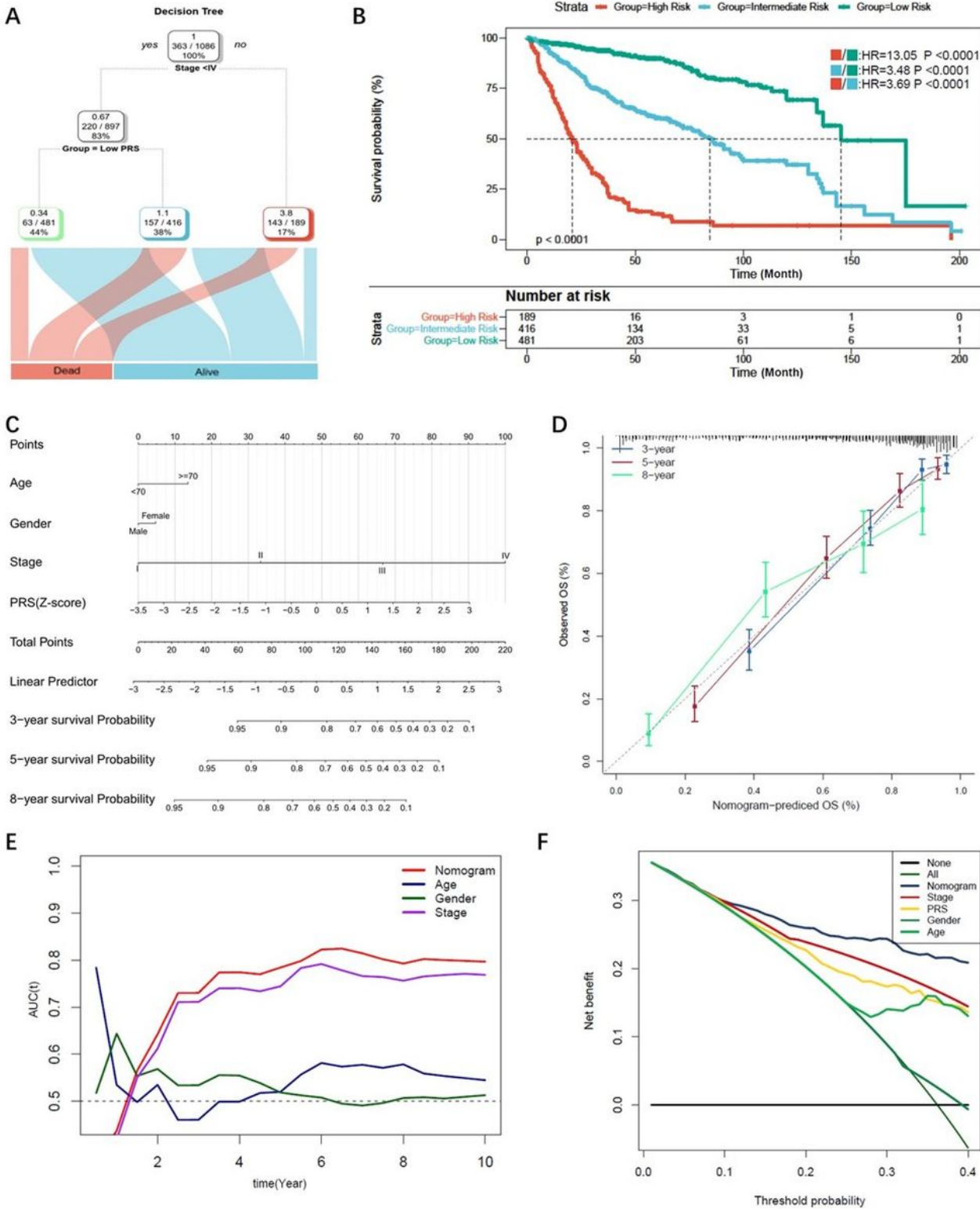


Figure 7

Combination of the pyroptosis signature and clinicopathological features improves risk stratification and survival prediction. (A) A decision tree was constructed to improve risk stratification. (B) Performance of the decision tree. (C) A nomogram was constructed to quantify risk assessment for individual patients.

(D) Calibration analysis indicated a high accuracy of survival prediction. (E, F) tROC analysis and decision curve analysis (DCA) demonstrated that the nomogram was the most stable and powerful predictor for OS among all the clinical variables.

Supplementary Files

This is a list of supplementary files associated with this preprint. Click to download.

- [SupplyFigure1.jpg](#)
- [SupplyFigure2.jpg](#)